

Efficient MAPbI₃ solar cells made *via* drop-coating at room temperature

Lixiu Zhang^{1,2}, Chuantian Zuo^{1,†}, and Liming Ding^{1,†}

¹Center for Excellence in Nanoscience (CAS), Key Laboratory of Nanosystem and Hierarchical Fabrication (CAS), National Center for Nanoscience and Technology, Beijing 100190, China

²University of Chinese Academy of Sciences, Beijing 100049, China

Abstract: Here we demonstrate a room-temperature drop-coating method for MAPbI₃ films. By using low-boiling-point solvent, high-quality MAPbI₃ films were made by simply casting a drop of solution onto the substrate at room temperature. This approach took advantage of the synergistic effect of good wettability and volatility of the solvent, enabling high nuclei density and compact film at room temperature. The crystal growth in different solvents was *in-situ* observed by using optical microscope, which helped us to understand the mechanism for the formation of different film morphology. Perovskite solar cells gave a PCE of 18.21%.

Key words: perovskite solar cells; drop-coating; room temperature; low-boiling-point solvent; crystal growth

Citation: L X Zhang, C T Zuo, and L M Ding, Efficient MAPbI₃ solar cells made *via* drop-coating at room temperature[J]. *J. Semicond.*, 2021, 42(7), 072201. <http://doi.org/10.1088/1674-4926/42/7/072201>

1. Introduction

Perovskite solar cells have been recognized as competitive candidates for the next-generation photovoltaics because of their superior performance, solution processibility, and low cost^[1–3]. The state-of-the-art power conversion efficiency (PCE) for lab cells has been promoted to 25.5%^[4], motivating the exploration of upscaling and commercialization. Up to now, most of the top-performing perovskite solar cells are made by spin-coating assisted with Lewis acid-base adduct and anti-solvent^[1–3], which is not suitable for large-scale manufacturing due to the large material waste, the narrow processing window, and the operation difficulty in anti-solvent dripping. Alternatively, various scalable deposition methods have been developed, e.g. slot-die coating^[5, 6], blade coating^[7, 8], bar coating^[9], spray coating^[10], etc. However, unlike the centrifugal-force-driven film formation in spin-coating, the drying process of the above methods is slower, resulting in different crystallization process. To obtain high-quality perovskite films, heating, gas blowing, or vacuum treatment are often used in the above methods to regulate crystal growth. Achieving high-quality films *via* a natural drying process will greatly simplify the preparation process and reduce cost.

We ever reported a facile drop-coating method, and high-quality perovskite films can form spontaneously from a drop of solution on heated substrates^[11–14]. In that method, DMF/DMSO mixed solvent and two-step heating process were required to obtain high-quality MAPbI₃ films^[13]. Making perovskite films at room temperature is highly desirable in order to save energy and further reduce cost. The low-boiling-point solvent system, methylamine (MA) solution in acetonitrile (ACN), is feasible for room-temperature crystallization, which has been utilized in spin-coating^[15] and blade coating^[16, 17]. However, MA solution in ACN needs to be prepared with a gas-bubbling method^[15, 17], which is complicated and hard to give an accurate MA : ACN ratio. Using purchasable MA solution in ethanol (EtOH) as MA source can simplify the processing.

Herein, we present a room-temperature drop-coating method to produce MAPbI₃ films. A low-boiling-point solvent containing MA (boiling point: –6.3 °C), EtOH (boiling point: 78 °C), and ACN (boiling point: 81.6 °C) was used, which enabled the preparation of high-quality films *via* drying naturally at room temperature. The effect of solvent on nucleation and growth of perovskite crystals was investigated by using *in-situ* optical microscopy. A mechanism for the formation of different film morphology is proposed. The solar cells made under ambient conditions gave a PCE of 18.21%.

The schematic diagram for the coating process is shown in Fig. 1(a). A drop of precursor solution (the preparation process, see Fig. S1) was cast onto a room-temperature substrate coated with PEDOT:PSS. The drying process can be divided into three stages. At stage 1, the good wettability of the solution on substrate enables self-spreading, yielding a light-yellow wet film. Whereafter, the solvents evaporate and dynamic interference rings can be observed (stage 2), indicating the thinning of the film. At stage 3, the film turns black, suggesting the beginning of crystal nucleation and growth. After drying, the film is annealed at 110 °C for 1 min to further promote crystallization. The drying processes of the solution with conventional DMF/DMSO solvent and MA(EtOH)/ACN solvent were recorded and presented in Figs. 1(b) and 1(c), respectively. Owing to the high boiling-point of DMF (153 °C) and DMSO (189 °C), the drying of DMF/DMSO solution was very slow (> 10 min). In comparison, it took only

2. Processing route of perovskite films

trile (ACN), is feasible for room-temperature crystallization, which has been utilized in spin-coating^[15] and blade coating^[16, 17]. However, MA solution in ACN needs to be prepared with a gas-bubbling method^[15, 17], which is complicated and hard to give an accurate MA : ACN ratio. Using purchasable MA solution in ethanol (EtOH) as MA source can simplify the processing.

Correspondence to: C T Zuo, zuocht@nanoctr.cn; L M Ding, ding@nanoctr.cn

Received 12 APRIL 2021.

©2021 Chinese Institute of Electronics

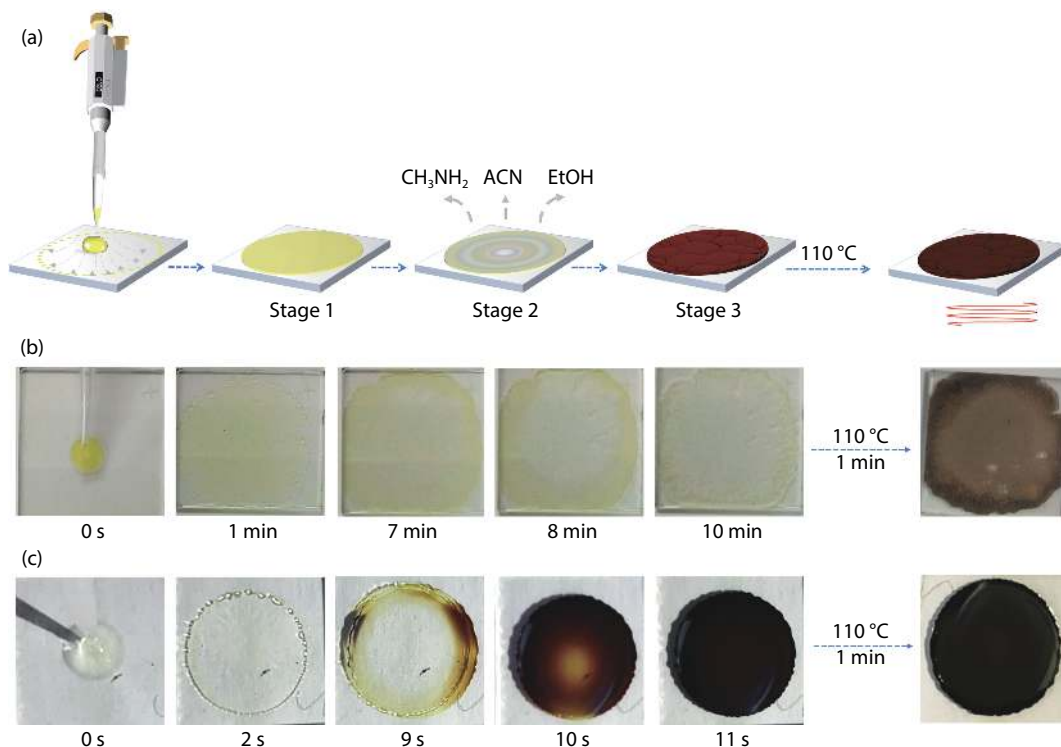


Fig. 1. (Color online) (a) Schematic illustration of the drop-coating method. (b) and (c) Video images for the drying process of MAPbI_3 solution with (b) DMF/DMSO solvent and (c) MA(EtOH)/ACN solvent.

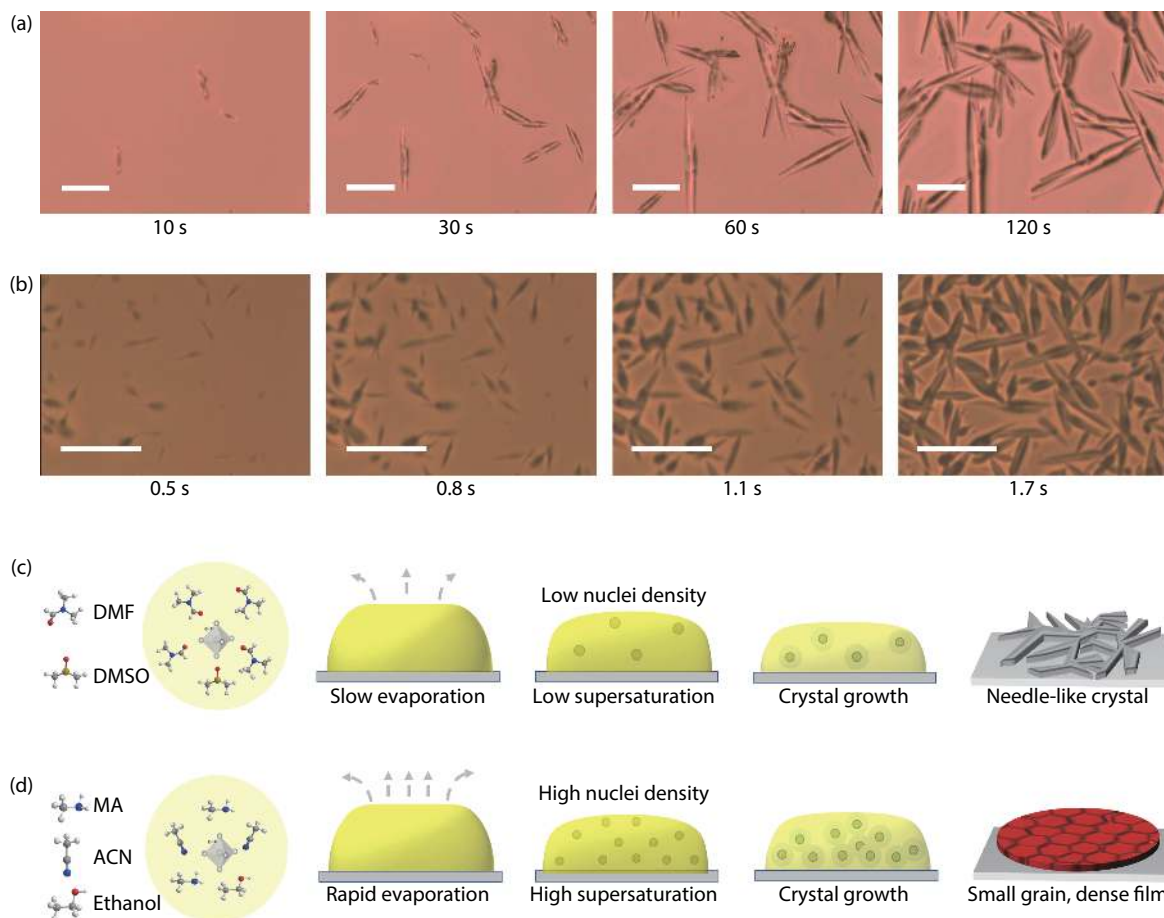


Fig. 2. (Color online) (a) and (b) Video images from the drying processes of (a) DMF/DMSO solution and (b) DMF solution. Scale bar: $30 \mu\text{m}$. (c) and (d) Illustration of the crystal growth in (c) high-boiling-point DMF/DMSO solution and (d) low-boiling-point MA(EtOH)/ACN solution.

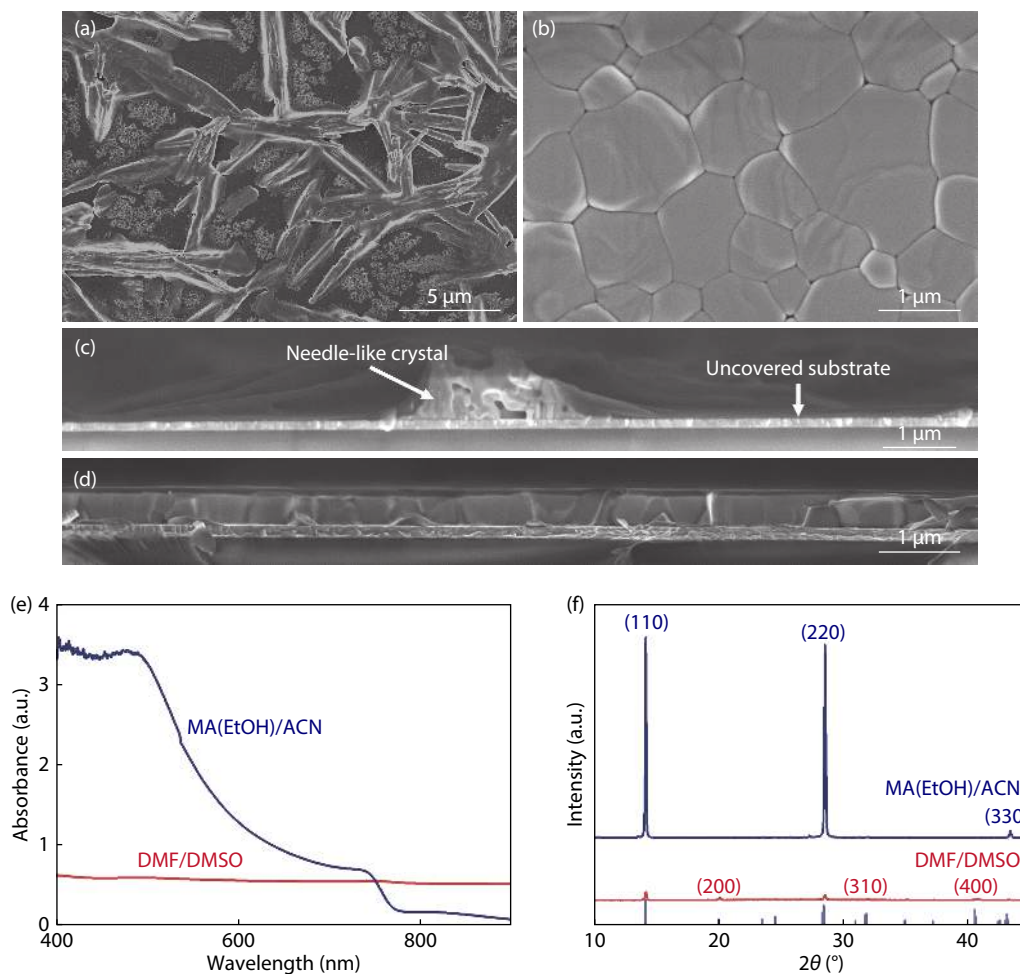


Fig. 3. (Color online) (a) and (b) SEM images (top view) for MAPbI₃ films made from (a) DMF/DMSO and (b) MA(EtOH)/ACN solutions. (c) and (d) Cross-sectional SEM images for MAPbI₃ films from (c) DMF/DMSO and (d) MA(EtOH)/ACN solutions. (e) UV-Vis absorption spectra and (f) XRD patterns for MAPbI₃ films from DMF/DMSO and MA(EtOH)/ACN solutions. The calculated pattern for MAPbI₃ powder is presented at the bottom.

11 s for MA(EtOH)/ACN solution to dry. Most importantly, the annealed film from MA(EtOH)/ACN solution is much smoother and more uniform than the film from DMF/DMSO solution.

3. *In-situ* crystal growth study and mechanism analysis

To investigate the effect of solvents on film morphology, the crystal growth processes were tracked by using optical microscope. For DMF/DMSO solution, the crystal growth lasted for more than 110 s due to the slow drying speed of the solvent (Fig. 2(a)). For DMF solution, the lower boiling-point of DMF results in much faster drying speed. The crystal growth finished in 2 s (Fig. 2(b)). The crystallization process of MA(EtOH)/ACN solution is too fast (< 0.5 s) for the camera to capture. Quite distinct film morphology was observed for the films made with different solvents (Fig. S2). The film from DMF/DMSO solution consisted of needle-like crystals. While the film from MA(EtOH)/ACN solution consisted of small grains. Other differences induced by solvents are nuclei density and crystal size. For DMF/DMSO solution, DMF solution, and MA(EtOH)/ACN solution, the nuclei densities are ~600, ~12500, and $\sim 1 \times 10^6 \text{ mm}^{-2}$ (estimated from optical microscopy images), with crystal sizes of ~90, ~25, and ~1 μm , respectively. The nuclei density increases as boiling-point decreases, leading to decreased crystal size and increased sub-

strate coverage.

LaMer model^[18] can be used to explain the above different film morphology, and it divides the crystallization process into three stages (Fig. S3): (i) The concentration increases as the solvent evaporates; (ii) nucleation starts when the concentration reaches the threshold value $C_{\text{nucleation}}$ of supersaturation; (iii) diffusion-controlled crystal growth starts from nuclei. For the solution with high-boiling-point solvent (Fig. 2(c)), the slow evaporation rate causes a low degree of supersaturation, slow nucleation and low nuclei density, thus leading to the formation of sparse needle-like crystals. For the solution with low-boiling-point solvent (Fig. 2(d)), the rapid evaporation induces a high degree of supersaturation and high nuclei density, which limits the overgrowth from minor nuclei, leading to a compact film with closely packed grains.

4. Film morphology and quality characterization

The top-view scanning electron microscopy (SEM) images (Figs. 3(a) and 3(b)) for the films are consistent with the optical microscopy images. The film made from MA(EtOH)/ACN solution is compact with an average grain size of ~1.5 μm . The film from DMF/DMSO solution shows very uneven thickness and poor coverage (Fig. 3(c)). In contrast, the film from MA(EtOH)/ACN solution presents a uniform thick-

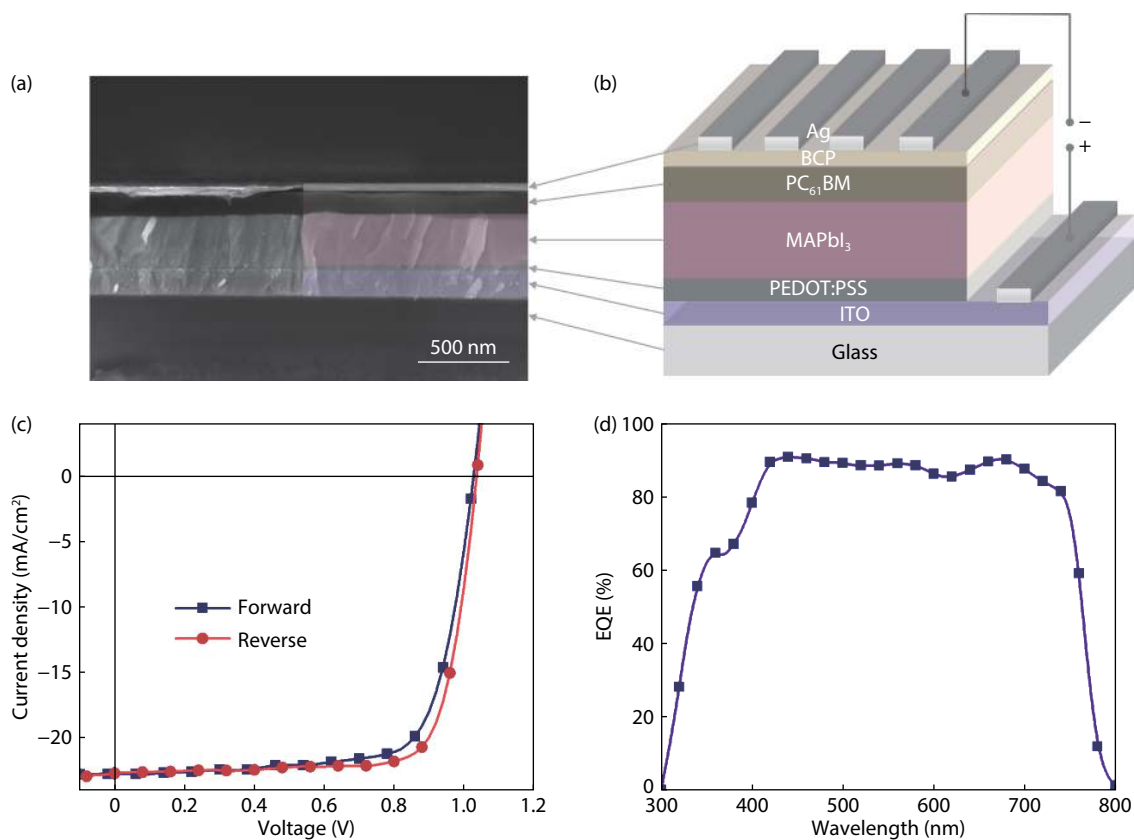


Fig. 4. (Color online) (a) Cross-sectional SEM image for the cell made with MA(EtOH)/ACN solution. (b) Device structure. (c) J - V curves under forward and reverse scans. (d) EQE spectrum for the best cell.

Table 1. Performance data for the best cell.

Parameter	V_{oc} (V)	J_{sc} (mA/cm ²)	FF (%)	PCE (%)
Reverse	1.04	22.70	77.39	18.21
Forward	1.03	22.74	73.48	17.17

ness and a high degree of flatness over a range of 11 μm , with no lateral grain boundaries (Fig. 3(d)). The pinhole-free, compact, and uniform morphology results in good light absorption (Fig. 3(e)). The good film morphology also ensures efficient charge transport at interfaces and reduces recombination, eventually leading to enhanced device performance.

The X-ray diffraction (XRD) patterns for the perovskite films are presented in Fig. 3(f). The film made from DMF/DMSO solution shows multiple peaks corresponding to (110), (200), (220), (310), and (400) planes. While the film from MA(EtOH)/ACN solution shows only parallel (110), (220), and (330) planes, with very high intensity. The much higher intensity ratio of (110) plane to other planes indicates a preferred (110) orientation.

5. Photovoltaic performance

MAPbI₃ solar cells were made with the drop-coated films (Fig. 4). The cells made with DMF/DMSO solution were short due to the low coverage of perovskite films (Fig. 3(c)). Compact and uniform MAPbI₃ layer with a thickness of ~ 300 nm can be seen clearly in the cross-sectional SEM image of the device (Fig. 4(a)). The best cell gave a PCE of 18.21% (reverse scan), with minor hysteresis (Fig. 4(c) and Table 1). The J_{sc} of 22.70 mA/cm² from J - V curve is consistent with the integrated current density (21.56 mA/cm²) from EQE spectrum.

6. Conclusion

The drop-coating method was used to prepare MAPbI₃ films in ambient air. Owing to the low-boiling-point of MA(EtOH)/ACN solvent, high-quality MAPbI₃ films can form spontaneously from a drop of solution without the assistance of heating, gas blowing, or antisolvent, which are yet indispensable for other coating methods. The formation mechanism for the different morphology of the films made with different solvents was investigated by using *in-situ* optical microscopy. The fast evaporation of volatile solvent induced high nuclei density and suppressed the overgrowth from minor nuclei, yielding a dense and uniform film with closely packed grains. The solar cells gave a PCE of 18.21%.

Acknowledgements

We thank the National Key Research and Development Program of China (2017YFA0206600) and the National Natural Science Foundation of China (51773045, 21772030, 51922032 and 21961160720) for financial support.

Appendix A. Supplementary materials

Supplementary materials to this article can be found online at <https://doi.org/1674-4926/42/7/072201>.

References

- [1] Yoo J J, Seo G, Chua M R, et al. Efficient perovskite solar cells *via* improved carrier management. *Nature*, 2021, 590, 587
- [2] Jeong M, Choi I W, Go E M, et al. Stable perovskite solar cells with efficiency exceeding 24.8% and 0.3 V voltage loss. *Science*, 2020,

369, 1615

- [3] Kim G, Min H, Lee K S, et al. Impact of strain relaxation on performance of α -formamidinium lead iodide perovskite solar cells. *Science*, 2020, 370, 108
- [4] Best research-cell efficiencies. <https://www.nrel.gov/pv/assets/pdfs/best-research-cell-efficiencies.20200104.pdf>
- [5] Du M, Zhu X, Wang L, et al. High-pressure nitrogen-extraction and effective passivation to attain highest large-area perovskite solar module efficiency. *Adv Mater*, 2020, 32, 2004979
- [6] Subbiah A S, Isikgor F H, Howells C T, et al. High-performance perovskite single-junction and textured perovskite/silicon tandem solar cells via slot-die coating. *ACS Energy Lett*, 2020, 5, 3034
- [7] Chen S, Xiao X, Gu H, et al. Iodine reduction for reproducible and high-performance perovskite solar cells and modules. *Sci Adv*, 2021, 7, eabe8130
- [8] Wu W Q, Rudd P N, Ni Z, et al. Reducing surface halide deficiency for efficient and stable iodide-based perovskite solar cells. *J Am Chem Soc*, 2020, 142, 3989
- [9] Jeong D N, Lee D K, Seo S, et al. Perovskite cluster-containing solution for scalable D-bar coating toward high-throughput perovskite solar cells. *ACS Energy Lett*, 2019, 4, 1189
- [10] Bishop J E, Read C D, Smith J A, et al. Fully spray-coated triplecation perovskite solar cells. *Sci Rep*, 2020, 10, 6610
- [11] Zuo C, Scully A D, Tan W L, et al. Crystallisation control of drop-cast quasi-2D/3D perovskite layers for efficient solar cells. *Commun Mater*, 2020, 1, 33
- [12] Zuo C, Scully A, Yak D, et al. Self-assembled 2D perovskite layers for efficient printable solar cells. *Adv Energy Mater*, 2019, 9, 1803258
- [13] Zuo C, Ding L. Drop-casting enables making efficient perovskite solar cells under high humidity. *Angew Chem Int Ed*, 2021, 60, 11242
- [14] Xiao H, Zuo C, Liu F, et al. Drop-coating produces efficient CsPbI₂Br solar cells. *J Semicond*, 2021, 42, 050502
- [15] Noel N K, Habisreutinger S N, Wenger B, et al. A low viscosity, low boiling point, clean solvent system for the rapid crystallisation of highly specular perovskite films. *Energy Environ Sci*, 2017, 10, 145
- [16] Wang K, Wu C, Hou Y, et al. Isothermally crystallize perovskites at room-temperature. *Energy Environ Sci*, 2020, 5, 3034
- [17] Dou B, Whitaker J B, Bruening K, et al. Roll-to-roll printing of per-

ovskite solar cells. *ACS Energy Lett*, 2018, 3, 2558

- [18] Chu D B K, Owen J S, Peters B. Nucleation and growth kinetics from laser burst data. *J Phys Chem A*, 2017, 121, 7511



Lixiu Zhang got her BS degree from Soochow University in 2019. Now she is a PhD student at University of Chinese Academy of Sciences under the supervision of Prof. Liming Ding. Her research focuses on perovskite solar cells.



Chuantian Zuo received his PhD degree in 2018 from National Center for Nanoscience and Technology (CAS) under the supervision of Professor Liming Ding. Then he did postdoctoral research in CSIRO, Australia. Currently, he is an assistant professor in Liming Ding Group. His research focuses on innovative fabrication techniques for perovskite solar cells.



Liming Ding got his PhD from University of Science and Technology of China (was a joint student at Changchun Institute of Applied Chemistry, CAS). He started his research on OSCs and PLEDs in Olle Inganäs Lab in 1998. Later on, he worked at National Center for Polymer Research, Wright-Patterson Air Force Base and Argonne National Lab (USA). He joined Konarka as a Senior Scientist in 2008. In 2010, he joined National Center for Nanoscience and Technology as a full professor. His research focuses on functional materials and devices. He is RSC Fellow, the nominator for Xplorer Prize, and the Associate Editors for Science Bulletin and Journal of Semiconductors.